Journal of Science: Advanced Materials and Devices 1 (2016) 61–64

Contents lists available at ScienceDirect

Journal of Science: Advanced Materials and Devices

journal homepage: www.elsevier.com/locate/jsamd

Original article

Cascaded plasmon resonant field enhancement in protein-conjugated gold nanoparticles: Role of protein shell

Anh D. Phan*, Trinh X. Hoang

Institute of Physics, Vietnam Academy of Science and Technology, 10 Dao Tan, Hanoi, 10000, Viet Nam

ARTICLE INFO

Article history:
Received 2 March 2016
Accepted 10 March 2016
Available online 11 April 2016

ABSTRACT

We study the cascaded plasmon resonant field enhancement in core–shell nanoparticles using the coupled dipole method. It is found that internal field inside protein-conjugated gold nanoparticles remains constant for large wavelengths of light but is significantly enhanced at 5944 nm due to the screening from the protein shell. The maximum ratio of the internal field to the incident field can reach up to 12. Effects from surrounding nanoparticles on the peak position in the internal field spectra are relatively weak. These findings pave a pathway for designing the state-of-the-art biosensing based on plasmonic-nanoantenna in infrared regime.

1. Introduction

The rapid advances in nanotechnology have created new opportunities for the high accuracy fabrication of nano devices and nano systems. Researchers studying the strong interactions in nano systems, particularly the plasmonic resonances of composite nanoparticles, have discovered new phenomena applicable in a large variety of fields ranging from physics and chemistry to biology [1,2]. In this science, metallic nanoparticles are a topic of great interest for both experimentalists and theoreticalists.

Recently, the conjugation between bovine serum albumin (BSA) proteins and gold nanoparticles has been intensively studied due to its various applications, particularly in medicine. The BSA layer on the gold surfaces consisting of sulphur, oxygen and nitrogen atoms allows gold nanoparticles to stabilize in solution [3]. The biocompatibility of BSA with other unhealthy cells can be exploited to design drug delivery vehicles. Once gold nanoparticles are delivered to the location of damaged cells, one can exploit optical properties such as plasmonics to detect diseases in early stage [4,5] and destroy cancer cells [6] based on the photothermal effect of gold nanoparticles. Additionally, it was found that gold nanoparticles can penetrate membrane without damaging cells [7]. This finding suggests it is possible to kill locally unhealthy cells from inside without affecting healthy cells.

In this paper, we use the coupled dipole method (CDM) to study the variation of the internal field inside protein-conjugated nanoparticles. The CDM has been widely used to study the van der Waals interactions [8–10], near-field heat transfers [11,12], and plasmonic optical properties [13]. The approach considers atoms and nanoparticles in systems as dipoles interacting with each other. The effect of nanoparticle size is represented in the effective expressions of polarizability. Furthermore, the impact of the surrounding environment on the plasmonic properties is provided via the environmental dielectric function in the Green functions and the polarizabilities.

2. Theoretical background

In our calculations, we study the properties of BSA-coated gold nanoparticle systems. We consider the main interaction between two arbitrary nanoparticles as a dipole–dipole interaction. A description of the polarization of the dipole $\mathbf{p}_i$ at position $\mathbf{r}_i$ is given by Ref. [13].

$$\mathbf{p}_i = \alpha_i \mathbf{E}_{loc}(\mathbf{r}_i), \tag{1}$$

where $\mathbf{E}_{loc}(\mathbf{r}_i)$ is a sum of the external electric field $\mathbf{E}_0$ and the induced electric field $\mathbf{E}_i^{ind} = \mu_0\omega^2 \sum_{j\neq i} \mathbf{G}_{ij}\mathbf{p}_j$ caused by electromagnetic fluctuations of other dipoles [10], μ_0 is the vacuum permeability and $\mathbf{G}_{ij}$ is the Green's function for dipolar coupling when the

* Corresponding author.
E-mail address: adphan35@gmail.com (A.D. Phan).
Peer review under responsibility of Vietnam National University, Hanoi.

http://dx.doi.org/10.1016/j.jsamd.2016.03.002

system is irradiated by light polarized along the center–center line between dipole i and j. The expression of $\mathbf{G}_{ij}$ is written as the extended free-space Green function

$$\mathbf{G}_{ij} = \frac{e^{ikR_{ij}}}{4\pi R_{ij}}\left[\left(1+\frac{i}{kR_{ij}}-\frac{1}{k^2R_{ij}^2}\right)\mathbf{I} + \left(-1-\frac{3i}{kR_{ij}}+\frac{3}{k^2R_{ij}^2}\right)\hat{\mathbf{R}}_{ij}\otimes\hat{\mathbf{R}}_{ij}\right], \tag{2}$$

where $k=\omega\sqrt{\varepsilon_3}/c$ is the wave vector in medium, ε_3 is the dielectric function of the surrounding medium as described in Fig. 1, ε_0 is the vacuum permittivity, $\mathbf{R}_{ij}=\mathbf{r}_i-\mathbf{r}_j$, $\hat{\mathbf{R}}_{ij}=\mathbf{R}_{ij}/R_{ij}$, and $\mathbf{I}$ is the 3×3 identity matrix. In the case of nanoparticles located in a line and the incident light polarized along this line, $\mathbf{G}_{ij}$ can be rewritten as the Green function for one-dimensional systems

$$G_{ij} = \frac{e^{ikR_{ij}}}{2\pi k^2}\left(-\frac{ik}{R_{ij}^2}+\frac{1}{R_{ij}^3}\right). \tag{3}$$

α_i is the polarizability of the ith dipole. The polarizability of core–shell particles can be calculated using the Maxwell–Garnett theory for an effective medium approximation [14,15].

$$\begin{aligned}\alpha &= 4\pi\varepsilon_0\varepsilon_3 R_{out}^3\frac{\varepsilon_2\varepsilon_a-\varepsilon_3\varepsilon_b}{\varepsilon_2\varepsilon_a+2\varepsilon_3\varepsilon_b},\\ \varepsilon_a &= \varepsilon_1\left[1+2\left(\frac{R_{in}}{R_{out}}\right)^3\right]+2\varepsilon_2\left[1-\left(\frac{R_{in}}{R_{out}}\right)^3\right],\\ \varepsilon_b &= \varepsilon_1\left[1-\left(\frac{R_{in}}{R_{out}}\right)^3\right]+\varepsilon_2\left[2+\left(\frac{R_{in}}{R_{out}}\right)^3\right],\end{aligned} \tag{4}$$

in which ε_1 and ε_2 are the dielectric function for the core and shell, respectively. R_{in} is the radius of core and R_{out} is the radius of core–shell nanoparticle.

Eq. (1) can therefore be re-expressed as

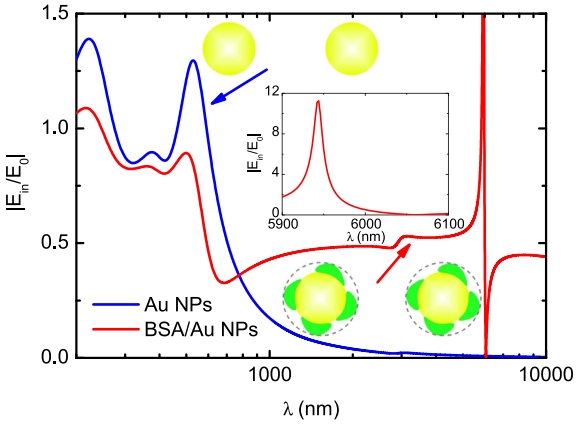

Fig. 1. Internal field spectra as a function of illumination wavelength at the center-to-center distance of 40 nm and gold particle radii of 10 nm.

$$\begin{aligned}\mathbf{p}_i &= \alpha_i\mathbf{E}_0+\alpha_i\mu_0\omega^2\sum_{j\neq i}G_{ij}\mathbf{p}_j\\ &= \alpha_i\mathbf{E}_0-\alpha_i\mu_0\omega^2\sum_{j\neq i}\frac{e^{ikR_{ij}}}{2\pi k^2}\left(\frac{ik}{R_{ij}^2}-\frac{1}{R_{ij}^3}\right)\mathbf{p}_j\\ &= \alpha_i\left[\mathbf{E}_0-\sum_{j\neq i}\frac{e^{ikR_{ij}}}{2\pi\varepsilon_0\varepsilon_3}\left(\frac{ik}{R_{ij}^2}-\frac{1}{R_{ij}^3}\right)\mathbf{p}_j\right]\\ &= \alpha_i\left[\mathbf{E}_0-\sum_{j\neq i}A_{ij}\mathbf{p}_j\right],\end{aligned} \tag{5}$$

where

$$A_{ij} = \frac{e^{ikR_{ij}}}{2\pi\varepsilon_0\varepsilon_3}\left(\frac{ik}{R_{ij}^2}-\frac{1}{R_{ij}^3}\right). \tag{6}$$

The result of Eq. (5) maintains good agreement with the finding in the consideration of nanoparticle dimers [13]. Recent theoretical [15] and experimental calculations show that BSA protein molecules form a non-complete monolayer on the surface of gold nanoparticles. The shell of protein-BSA-coated gold nanoparticles, consequently, must consist of water and proteins. The dielectric function of the shell can be expressed by Ref. [15].

$$\varepsilon_2 = f\varepsilon_{protein}+(1-f)f\varepsilon_3, \tag{7}$$

where $\varepsilon_{protein}$ is the dielectric function of BSA protein and f is the fraction of protein in the shell. For metallic nanoparticles with radii ranging from 8 to 50 nm, $f=0.4$, as found in the reference [15]. Parameters and models of ε_1 and $\varepsilon_{protein}$ can be easily found in previous studies [15,17,16]. The dielectric function of gold nanoparticles and medium versus frequency is described by the Lorentz-Drude model [18].

$$\varepsilon_{1,3}(\omega) = 1-\frac{f_0\omega_p^2}{\omega(\omega+i\gamma_0)}+\sum_s\frac{C_s}{\omega_s^2-i\omega\gamma_s-\omega^2}, \tag{8}$$

where ω_s is the resonant frequency, γ_s is the damping parameter, and C_s is oscillatory strength. All parameters can be found in Table 1.

3. Results and discussions

The dipole model has been shown to only be valid when the distances between two nanoparticles is at least twice as large as the radii [19]. We, therefore, choose center-to-center distances that allow for the reasonable use of the dipolar approach. In a system of two nanoparticles, one can find that [13].

$$\frac{E_{1,in}}{E_0} = \frac{3\varepsilon_3}{\varepsilon_{1,p}+2\varepsilon_3}\frac{1-\alpha_2A_{12}}{1-\alpha_2A_{12}\alpha_1A_{21}}, \tag{9}$$

where $E_{1,in}$ is the electric field inside the first nanoparticle and $\varepsilon_{1,p}$ is the dielectric function of nanoparticle 1. For uncoated nanoparticles, $\varepsilon_p=\varepsilon_1$. For protein-coated nanoparticles, $\varepsilon_p=\varepsilon_2\varepsilon_a/\varepsilon_b$. Calculating the interactions between two identical nanoparticles suggests $\alpha_1=\alpha_2$ and $A_{12}=A_{21}$. Eq. (9) can be recasted as

$$\frac{E_{1,in}}{E_0} = \frac{3\varepsilon_3}{\varepsilon_p+2\varepsilon_3}\frac{1}{1+\alpha_1A_{21}}. \tag{10}$$

As we can see in Fig. 1, the protein shell has a significant influence on the localized field inside nanoparticles. When $\lambda\leq800$ nm,

Table 1
Parameters for dielectric functions of AuNP, water and BSA protein provided in Ref. [16–18]–.

Parameter	AuNP	Water	BSA
f_0	0.76	–	–
γ_0 (eV)	0.053	–	–
ω_p (eV)	9.03	–	–
C_1 (eV^2)	1.957	6.3 × 10−4	0.0131
γ_1 (eV)	0.241	1.5 × 10−2	0
ω_1 (eV)	0.415	2.1 × 10−2	0.205
C_2 (eV^2)	0.815	3.5 × 10−3	2.0
γ_2 (eV)	0.345	3.8 × 10−2	0.5
ω_2 (eV)	0.830	6.9 × 10−2	6.4
C_3 (eV^2)	5.789	1.3 × 10−3	180
γ_3 (eV)	0.870	2.8 × 10−2	8
ω_3 (eV)	2.969	9.2 × 10−2	12.5
C_4 (eV^2)	49	5.4 × 10−4	225
γ_4 (eV)	2.494	2.5 × 10−2	19
ω_4 (eV)	4.304	0.2	21.5
C_5 (eV^2)	357.475	1.3 × 10−2	–
γ_5 (eV)	2.214	5.6 × 10−2	–
ω_5 (eV)	13.32	0.42	–
C_6 (eV^2)	–	2.156	–
γ_6 (eV)	–	0.5248	–
ω_6 (eV)	–	8.293	–
C_7 (eV^2)	–	5.184	–
γ_7 (eV)	–	0.8132	–
ω_7 (eV)	–	10.02	–
C_8 (eV^2)	–	11.66	–
γ_8 (eV)	–	1.768	–
ω_8 (eV)	–	11.46	–
C_9 (eV^2)	–	25.38	–
γ_9 (eV)	–	2.497	–
ω_9 (eV)	–	13.15	–
C_{10} (eV^2)	–	33.65	–
γ_{10} (eV)	–	3.922	–
ω_{10} (eV)	–	14.74	–
C_{11} (eV^2)	–	95.86	
γ_{11} (eV)	–	7.192	–
ω_{11} (eV)	–	18.18	–

the internal field of the gold nanoparticles is greater than that of the protein-coated gold nanoparticles. The three local maxima in the two curves are due to the plasmonic properties of the gold nanoparticles in this region. For larger wavelengths ($\lambda \geq 1000$ nm), the internal field of the gold nanoparticles decreases dramatically. The screening of the protein layer is responsible for keeping the field of the gold nanoparticles unchanged. Interestingly, we can observe the cascaded plasmon resonant field enhancement in protein-coated nanoparticles. $|E_{in}/E_0|$ reaches nearly 12 at approximately 5944 nm.

One salient feature of the internal field spectrum of BSA-coated gold nanoparticles is the strong peak around 6000 nm, shown in Fig. 1. This peak results from the low frequency resonances of the BSA protein. In particular, the lowest resonant frequency of BSA is $\omega_1 = 0.205\,eV$, which corresponds to a wavelength of 6049 nm. The second peak, at approximately 3000 nm, is due to $\omega_1 = 0.415$ eV of gold nanoparticles. Note that $\omega_1 = 0.205$ eV has $\gamma_1 = 0$ for BSA protein, while $\omega_1 = 0.415$ eV has $\gamma_1 = 0.241$ eV for gold nanoparticles. The second gamma is quite large. These findings explain why we observe a very sharp resonance at the first omega, while only a very small resonance at the second omega with the very large gamma. The interactions between the metallic particles and the BSA protein cause the blue-shifts of the peak positions compared to the isolation cases. The expression of ε_p of protein-coated nanoparticles presents a mutual impact of the components. For low frequencies, the peaks in the field enhancement correspond close to the resonant frequencies of the materials involved, while at higher frequencies, the peaks correspond more loosely to such resonances.

At low frequencies, $\omega \approx 0$, $\varepsilon_p = \varepsilon_p(0)$ for metallic particles. The dielectric function of metals is usually described by the Drude or plasma model and the Lorentz-Drude model for metallic particles. All descriptions agree that $\varepsilon_p(0) = \infty$. The combination of this result and Eq. (10) points out that $E_{1,in} \rightarrow 0$ at low frequencies or large wavelengths. The finding explains the shape of the curve corresponding to AuNPs in Fig. 1. However, $\varepsilon_p(0) \neq 0$ for dielectric materials. Therefore, $E_{1,in}/E_0 = constant \neq 0$ in the case of protein-coated NPs.

To determine the many-body effects induced by the second particle, we calculate the variation of the internal field inside a particle as a function of center-to-center distances. As seen in Fig. 2, the presence of the second particle induces the red shift of plasmonic peaks compared to the case of the single particle. The maximum position moves from 5944 nm at $d = 40$ nm to 5941 and 5940 nm at $d = 60$ and 100 nm, respectively. The finding also suggests that for $d \geq 100$ nm, the particles are almost unaffected by each other. As a result, the systems of these complex particles can be treated as a collection of discrete particles in a dilute solution with the concentration $C < 10^{15}$ particles/ml. In previous studies [15,20], the concentration of the solution of protein-conjugated gold nanoparticles measured and calculated is smaller than 10^{13} particles/ml. Therefore, in practice, synthesized solutions are always dilute enough to ignore the inter-particle influences on optical properties (see Fig. 3).

One can also determine the effect of numerous nanoparticles on a nanoparticle by means of the Clausius-Mossotti approximation [21]. The effective polarizability of nanoparticle including many-body effects is given by

$$\alpha'(\lambda) = \frac{\alpha}{1 - N\alpha/3}, \tag{11}$$

where N is the density number of nanoparticles. When we consider a solution of BSA-coated nanoparticles with the concentration less than 10^{15} particles/ml, it means $N < 10^{21}$ particles/m^3. Since $4\pi NR_{out}^3/3 < 10^{-2}$, $N\alpha/3$ is quite small and we can approximate $\alpha' \approx \alpha$. This result is consistent with that obtained by the two-dipoles method.

The field enhancement of the nanocomposites is strongly dependent on their size. An increase of the nanoparticle radius causes a blue shift of the optical peak position and the reduction of $|E_{in}/E_0|$ in the infrared regime. The resonance position moves from 5940.7 nm to 5901 nm at considered values of R. A recent study [22] has shown that the diameter of nanoparticles less than 100 nm can

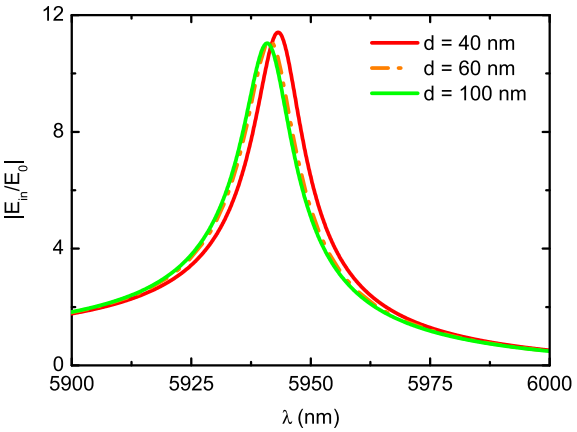

Fig. 2. Internal field spectra as a function of illumination wavelength at different center-to-center distances and gold particle radii of 10 nm.

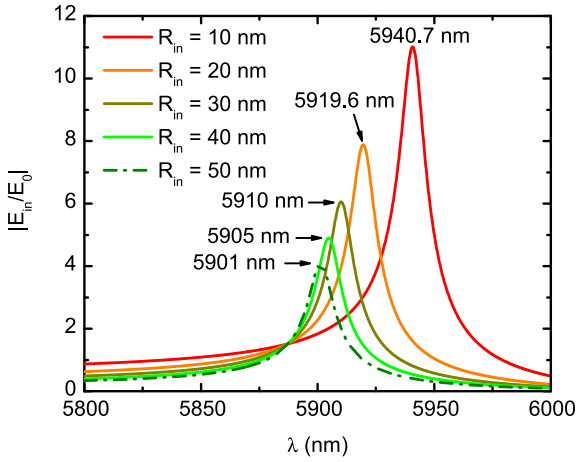

Fig. 3. Internal field spectra for an insolated gold nanoparticle in the infrared regime at different sizes.

be effectively used to destroy unhealthy cells without damaging membrane of healthy cells. Lagos and co-workers [23] found that $f \approx 0.4$ for gold nanoparticle with $R = 10–60$ nm. Eqs. (4) and (9) show that R_{in}/R_{out} is a decisive factor for $|E_{in}/E_0|$. As R_{in} increases, $R_{in}/R_{out} \to 1$ and $\varepsilon_p \to \varepsilon_1$ because $R_{out} = R_{in} + 3.35$ nm. This finding reveals that the field enhancement for the BSA-conjugated gold nanoparticle is larger than $|E_{in}/E_0|$ for the uncoated gold nanoparticle. The field enhancement can be more explicitly observed at small particles. Small nanoparticles, therefore, can be exploited to be much better nanoantenna than large nanoparticles due to the substantial quantum confinement effect. In order to design such nanocomposites as nanoantennas with high sensitivity, $|E_{in}/E_0|$ is expected to be large.

4. Conclusions

We have shown the enhancement of the internal field inside protein-conjugated gold nanoparticles in comparison with their bare gold nanoparticles. This finding is very useful for designing nano-plasmonic antennas and biosensors in the infrared regime. We have also exploited the optical spectrum to detect metallic nanoparticles wrapped by proteins or biomolecules. Consequently, it is possible to control the amount of biocompatible materials with high accuracy.

Acknowledgements

This work was supported by the Vietnam National Foundation for Science and Technology Development (NAFOSTED) under Grant No. 103.01–2013.16.

References

[1] S.V. Boriskina, H. Ghasemi, G. Chen, Plasmonic materials for energy: from physics to applications, Mater. Today 13 (2013) 375–386.
[2] M.L. Juan, M. Righini, R. Quidant, Plasmonic materials for energy: from physics to applications, Nat. Photonics 5 (2011) 349–356.
[3] S.H. Brewer, W.R. Glomm, M.C. Johnson, M.K. Knag, S. Franzen, Probing BSA binding to citrate-coated gold nanoparticles and surfaces, Langmuir 21 (2005) 349–356.
[4] D. Rand, V. Ortiz, Y. Liu, Z. Derdak, J.R. Wands, M. Taticek, C. Rose-Petruck, Nanomaterials for X-ray imaging: gold nanoparticle enhancement of X-ray scatter imaging of hepatocellular carcinoma, Nano Lett. 11 (2011) 2678–2683.
[5] C.-C. Chien, H.-H. Chen, S.-F. Lai, Y. Hwu, C. Petibois, C.S. Yang, Y. Chu, G. Margaritondo, X-ray imaging of tumor growth in live mice by detecting gold-nanoparticle-loaded cells, Sci. Rep. 2 (2012) 610.
[6] S. Wang, K.-J. Chen, T.-H. Wu, H. Wang, W.-Y. Lin, M. Ohashi, P.-Y. Chiou, H.-R. Tseng, Photothermal effects of supramolecularly assembled gold nanoparticles for the targeted treatment of cancer cells, Angew. Chem. Int. 49 (2010) 3777–3781.
[7] R.C.V. Lehn, P.U. Atukorale, R.P. Carney, Y.-S. Yang, F. Stellacci, Irvine, A. Alexander-Katz, Effect of particle diameter and surface composition on the spontaneous fusion of monolayer-protected gold nanoparticles with lipid bilayers, Nano Lett. 13 (2013) 4060–4067.
[8] M.W. Cole, D. Velegol, H.-Y. Kim, A.A. Lucus, Nanoscale van der Waals interactions, Mol. Simul. 35 (2009) 849–866.
[9] Y.V. Shtogun, L.M. Woods, Many-Body van der Waals interactions between graphitic nanostructures, J. Phys. Chem. Lett. 1 (2010) 1356–1362.
[10] A.D. Phan, L.M. Woods, T.-L. Phan, Van der Waals interactions between graphitic nanowiggles, J. Appl. Phys. 113 (2013) 044308.
[11] P. Ben-Abdallah, S.-A. Biehs, K. Joulain, Many-body radiative heat transfer theory, Phys. Rev. Lett. 107 (2011) 114301.
[12] R. Messina, M. Tschikin, S.-A. Biehs, P. Ben-Abdallah, Fluctuation-electrodynamic theory and dynamics of heat transfer in systems of multiple dipoles, Phys. Rev. B 88 (2013) 104307.
[13] S. Toroghi, P.G. Kik, Cascaded plasmon resonant field enhancement in nanoparticle dimers in the point dipole limit, Appl. Phys. Lett. 100 (2012) 183105.
[14] Bohren, C. F., Huffman, D. R., 1998. Absorption and scattering of light by small particles.
[15] A.D. Phan, T.X. Hoang, T.H.L. Nghiem, L.M. Woods, Surface plasmon resonances of protein-conjugated gold nanoparticles on graphitic substrates, Appl. Phys. Lett. 103 (2013) 163702.
[16] C.M. Roth, B.L. Neal, A.M. Lenhoff, Van der Waals interactions involving proteins, Biophys. J. 70 (1996) 977–987.
[17] A.D. Rakic, A.B. Djurisic, J.M. Elazar, M.L. Majewski, Optical properties of metallic films for vertical-cavity optoelectronic devices, Appl. Opt. 37 (1998) 5271–5283.
[18] M. Elbaum, M. Schick, Application of the theory of dispersion forces to the surface melting of ice, Phys. Rev. Lett. 66 (1991) 1713.
[19] G. Domingues, S. Volz, K. Joulain, J.-J. Greffet, Heat transfer between two nanoparticles through near field interaction, Phys. Rev. Lett. 94 (2005) 085901.
[20] T.H.L. Nghiem, T.H. La, X.H. Vu, V.H. Chu, T.H. Nguyen, Q.H. Le, E. Fort, Q.H. Do, H.N. Tran, Synthesis, capping and binding of colloidal gold nanoparticles to proteins, Adv. Nat. Sci. Nanosci. Nanotechnol. 1 (2010) 025009.
[21] N. Lagos, N.M. Sigalas, E. Lidorikis, Theory of plasmonic near-field enhanced absorption in solar cells, Appl. Phys. Lett. 99 (2011) 063304.
[22] L. Tang, et al., Investigating the optimal size of anticancer nanomedicine, PNAS 111 (2014) 15344–15349.
[23] D.-H. Tsai, F.W. DelRio, A.M. Keene, K.M. Tyner, R.I. MacCuspie, T.J. Cho, M.R. Zachariah, V.A. Hackley, Adsorption and conformation of serum albumin protein on gold nanoparticles investigated using dimensional measurements and in situ spectroscopic methods, Langmuir 27 (2011) 2464–2477.